

Spectroscopy, upconversion dynamics, and applications of Er^{3+} -doped low-phonon materials

Angel J. Garcia-Adeva

*Departamento de Física Aplicada I, E.T.S. Ingeniería de Bilbao, Alda. Urquijo s/n, 48013 Bilbao, Spain**

In this work I summarize some of the recent work carried out by our group on the upconversion dynamics of Er^{3+} -doped potassium lead halide crystals, which possess very small phonons and present very efficient blue and green upconversion. Furthermore, a non-conventional application of these RE-doped low-phonon materials in optical refrigeration of luminescent solids is also discussed, paying especial attention to new pathways for optical cooling that include infrared-to-visible upconversion. Finally, I conclude with some hints of what I think it is the next step into improving the luminescence efficiency of solids: the use of RE-doped nanoscale photonic heterostructures for controlling the density of photonic states.

I. INTRODUCTION

Rare-earth-doped materials capable of converting infrared radiation into visible light in an efficient way are potential candidates for photonic applications in several areas such as color displays, sensors, detection of infrared radiation, and upconversion lasers¹. Indeed, upconversion luminescence is considered as a promising solution to obtain efficient visible lasers pumped by commercial infrared laser diodes. The main shortcoming for the development of such applications is the need of host materials with low-phonon energy that leads to a significant reduction of the multiphonon relaxation rates and, thus, allows for an increased lifetime of some excited levels that can relax radiatively or can store energy for further upconversion, cross-relaxation, or energy-transfer processes.

Efficient ir-to-vis upconversion and laser action has been demonstrated in chlorides, bromides, and iodides compounds doped with different RE ions^{7,8,9,10,11,12}. In this low-phonon-energy materials, due to very small multiphonon relaxation rates and the long lifetime of the $^4\text{I}_{9/2}$ level, this one acts as an intermediate state for upconversion, leading to a number upconversion mechanisms. For instance, blue, green, and red emissions from the $^2\text{H}_{9/2}$ level by sequential upconversion excitation from the $^4\text{I}_{9/2}$ level has been demonstrated. Unfortunately, one drawback of chloride and bromide systems is that these materials usually present poor mechanical properties, moisture sensitivity, and are difficult to synthesize. In this regard, an important advance in the search for new low-phonon-energy materials has been the identification of potassium lead halide crystals KPb_2X_5 ($\text{X}=\text{Cl}, \text{Br}$) as new low-energy phonon hosts for RE ions^{12,14,15,16,17,18,19,20}. These crystals are non-hygroscopic and readily incorporate RE. The maximum phonon energy are 203 cm^{-1} and 138 cm^{-1} for the KPb_2Cl_5 and KPb_2Br_5 crystals, respectively. These small phonons are the main reason why efficient ir-to-vis upconversion in Pr^{3+} -doped and Yb^{3+} - Pr^{3+} -codoped KPb_2Cl_5 , in Er^{3+} -doped KPb_2Cl_5 , Nd^{3+} -doped KPb_2Cl_5 , and Er^{3+} -doped KPb_2Br_5 has been recently found by our group and, also, why we have been able to use one of these matrices for laser cooling of luminescent

solids.

The structure of this paper is as follows: in the next section, I will briefly summarize the main features of the ir-to-vis upconversion processes found in these systems. Then, I will explain how these materials could be used for the development of optical refrigeration applications of luminescent solids. I will end up this work explaining how I think one can control, from a general perspective, the luminescence efficiency of these solids and, in particular, the cooling efficiency, by using photonic nanostructures doped with optically active ions (such as RE) as a substrate for these applications.

II. UPCONVERSION DYNAMICS OF RE-DOPED POTASSIUM LEAD HALIDE CRYSTALS

Single crystals of non-hygroscopic Er^{3+} -doped ternary potassium lead chloride (KPC) and bromide (KPB) grown by the Bridgman technique were investigated. The maximum Er^{3+} concentration of the samples was about 1.0%. Conventional absorption spectra between 175 and 3000 nm were performed with a Cary 5 spectrophotometer. The steady-state emission measurements were made with a Ti-sapphire ring laser 0.4 cm^{-1} linewidth as exciting light source. The excitation beam was focused on the crystal by using a 50 mm focal lens. The fluorescence was analyzed with a 0.25 m monochromator, and the signal was detected by a Hamamatsu R928 photomultiplier and finally amplified by a standard lock-in technique. Lifetime measurements were obtained by exciting the sample with a dye laser pumped by a pulsed nitrogen laser and a Ti-sapphire laser pumped by a pulsed frequency-doubled neodymium-doped yttrium aluminum garnet Nd:YAG laser 9 ns pulse width, and detecting the emission with Hamamatsu R928 and R5509-72 photomultipliers. The data were processed by a Tektronix oscilloscope.

It is experimentally found that efficient red, green, and blue upconverted emissions are observed when matrices of KPC and KPB doped with Er^{3+} –up to a 1.0 % concentration– are pumped with cw laser radiation

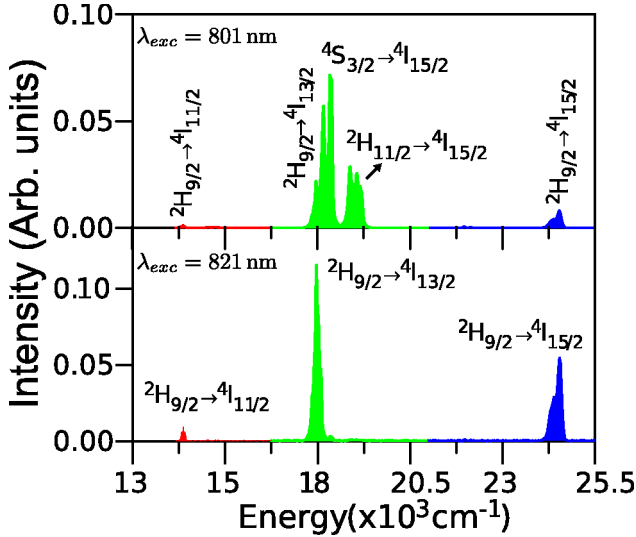


Figure 1: Er^{3+} -doped KPC upconverted emission spectra upon excitation at 801 nm (upper panel) and 821 nm (lower panel). The Er concentration was 0.5%.

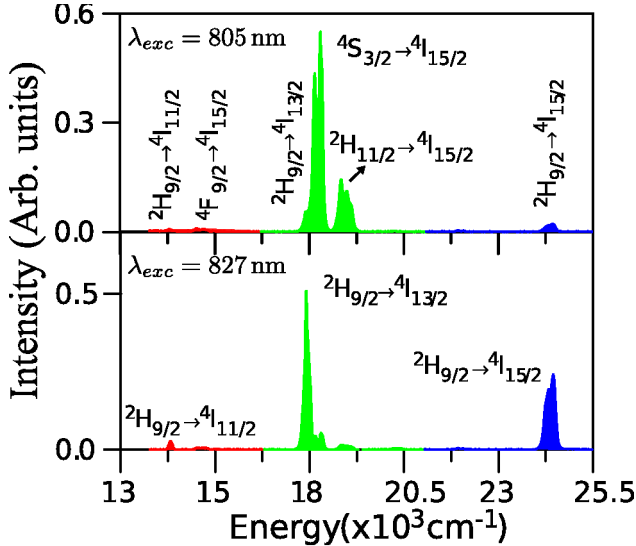


Figure 2: Er^{3+} -doped KPB upconverted emission spectra upon excitation at 805 nm (upper panel) and 827 nm (lower panel). The Er concentration was around 1.0%.

of an energy that corresponds to the energy difference between the $^4\text{I}_{9/2}$ manifold and the $^4\text{I}_{15/2}$ ground-state manifold. These results are summarized in figures 1 and 2 for the KPC and KPB systems, respectively. In particular, for the Er^{3+} -doped KPC when we pump resonantly with the barycenter of the $^4\text{I}_{9/2}$ level (801 nm), there are red, green, and blue upconverted emissions coming out from the $^2\text{H}_{9/2}$ and $^4\text{S}_{3/2}$ levels, as shown in the upper panel of figure 1. On the other hand, when we pump just below the $^4\text{I}_{9/2}$ level, we only get upconverted red, green, and blue emissions from the $^2\text{H}_{9/2}$ manifold, as can be seen in the lower panel of figure 1.

The situation is very similar in the case of the KPB compound (see fig. 2). The only difference is that there is also a small amount of red upconverted emission coming from the $^4\text{F}_{9/2}$ level when we excite resonantly into the $^4\text{I}_{9/2}$ level (upper panel in figure 2). The upconverted emission spectrum for non-resonant excitation just below this band, however, is totally analogous to the KPC case.

Apart from assessing the capability of these systems for efficient ir-to-vis upconversion, we were also very interested in elucidating the different mechanisms responsible for this upconversion. In this regard, a first clue to identify these is provided by the study of the power dependence of the upconverted emission intensity. The result of such a study shows that this quantity follows a power law dependence which is closer to a quadratic law rather than a linear one^{12,13}. This is a clear indication that two photons are involved in the upconversion process. Another useful tool to investigate this is the study of the upconverted population dynamics after pulsed excitation. This technique allows one to easily distinguish between an excited state absorption (ESA) process and an energy transfer upconversion (ETU) process²¹. In the first case, one electron in an excited state (the $^4\text{I}_{9/2}$ level, for example) absorbs a pumping photon and is promoted to a higher excited state (the $^2\text{H}_{9/2}$, for example). Later, when this electron decays spontaneously, it emits a photon of frequency twice the frequency of the pumping photons. In the second case, an electron in one ion initially in an excited state, decays spontaneously by exchanging a photon with a second electron in the same excited state of another ion and, thus, this later one is promoted to a higher excited state. Later, when this electron decays radiatively, it emits a photon of frequency twice the frequency of the incident photons. As said above, the population dynamics after pulsed excitation in these two cases is quite different. The typical signature of an ESA process is an exponential decay, whereas the signature of an ETU process is a rise followed by an exponential decay.

Experimentally, we find that, in the particular case of Er^{3+} -doped KPC, upon resonant excitation into the $^4\text{I}_{9/2}$ level (801 nm), we get a typical ETU behavior for both the blue and green upconverted emissions (see fig. 3a and 3b). The blue upconverted population initially increases and then it decays following a two-exponential behavior. The green upconverted population initially rises too and, then, it decays according to a single-exponential behavior. Even though I will not delve into these details here, it is important to stress that the rise and decay time constants are sub-multiples of the lifetimes of the levels involved in the upconversion processes. I refer the interested reader to references 12 and 13 for more details. On the other hand, the situation is radically different when we pump just below the $^4\text{I}_{9/2}$ level using a pumping frequency such that two pumping photons are in resonance with the $^2\text{H}_{9/2}$ level. Under this condition, the upconverted blue and green emissions show a clear ESA behavior (not shown here, see refs. 12 and 13 for details).

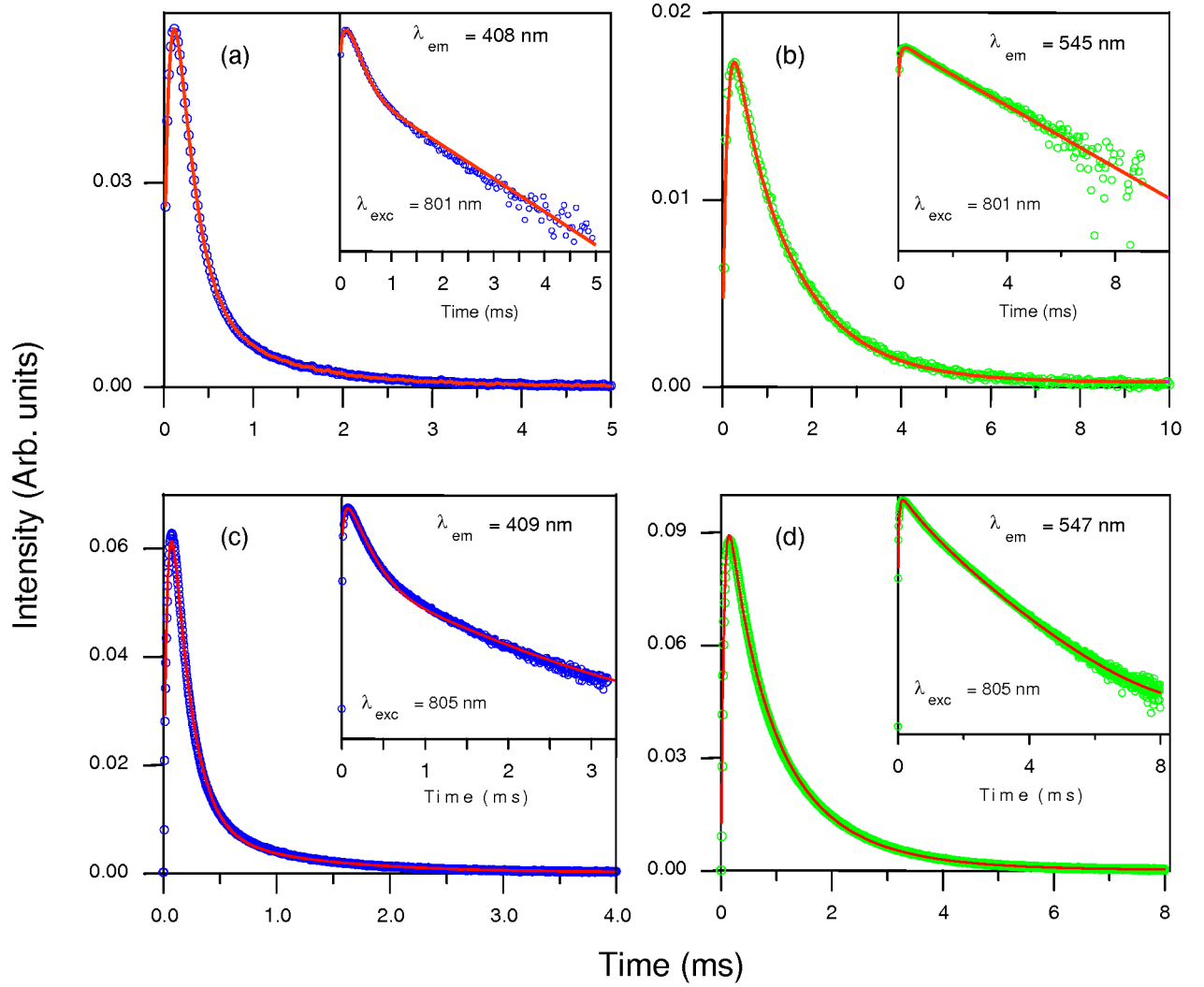


Figure 3: (a) Blue and (b) green upconverted emission intensity as a function of time for non-resonant excitation into the $^4\text{I}_{9/2}$ band together with the fit (solid lines) to our theoretical model for Er³⁺-doped KPC. (c) and (d): analogous to (a) and (b), respectively, for Er³⁺-doped KPB.

The results for the Er³⁺-doped KPB system are totally similar to the ones obtained for the KPC and can be seen in figure 3c and 3d.

In order to theoretically investigate the mechanisms responsible for the upconversion under non-resonant pumping, we performed a very simple rate equation analysis for both the KPC and KPB systems. The details of such approach can be found in refs. 12 and 13 and will be not reproduced here. For the present work, it suffices to say that the analytical expressions obtained in this way are in excellent agreement with the experimental data of the upconverted population dynamics, as can be seen in figures 3a and 3a and in figures 3c and 3d for both the blue and green upconverted emissions in Er³⁺-doped KPC and KPB, respectively. This, in turn, is a strong support for the validity of the proposed upconversion models.

III. LASER COOLING OF LUMINESCENT SOLIDS

In this section I will present a non-conventional application of the Er³⁺-doped low-phonon materials described in the previous section for the development of optical cryocoolers. The physics behind laser cooling of luminescent solids is based on what is known as an anti-Stokes transition²²: an optically active ion absorbs a photon from a pump laser beam and this excites an electron from the ground state manifold to the excited-state one. In the process, one or more phonons from the lattice are annihilated in order to make up for the energy mismatch between the pump photon energy and the excited state one. Later, when the electron decays spontaneously, it emits a fluorescence photon of frequency slightly larger than the pump one, so that in each of these events, a

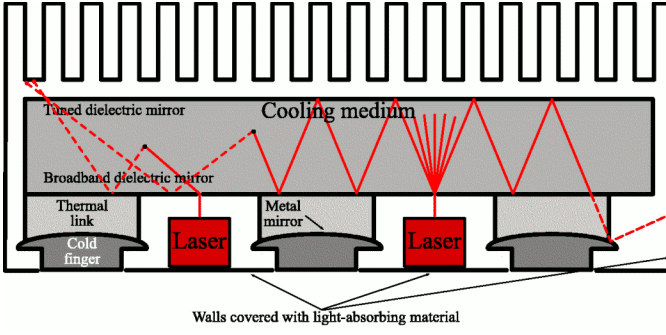


Figure 4: A proposed design for an optical cryocooler (based on a patent by Edwards et al., ref. 28).

small amount of thermal vibrational energy is removed from the system^{23,24,25}. Therefore, if this process occurs in a cyclic way, we have an optical refrigerator with a maximum theoretical cooling efficiency given by²⁴

$$\eta_{\text{cool}} = \frac{\nu_f - \nu_p}{\nu_p}. \quad (1)$$

Of course, this effect could have many applications²⁶. The simplest and probably most profitable one is for developing cryocoolers for the microprocessors of personal computers. Indeed, current generation CPU coolers have many mechanical parts and, thus, are subject to various shortcomings: they generate a lot of vibrations, they are noisy, and consume a lot of power. On the other hand, an optical cryocooler could look like the device shown in figure 4 (see refs. 27 and 28). It consists of an active medium that is pumped by a diode laser and which is linked to a cold finger that actually cools the CPU. The external walls of the device are covered with a special coating that absorbs any fluorescence escaping from the active medium. It is easy to realize that such a device would have many advantages: it has no mechanical parts and, thus, there are no vibrations, no noise, and –with the advent of the new generation diode lasers– it would consume very little power. Other important applications of this type of laser cooling are, for example, the development of radiation-balanced laser that use dual wavelength pumping to offset the heat generated by the pump laser. Also, this could have many applications in bioimaging and phototherapy, where this dual wavelength pumping could also partially offset the heat that could otherwise damage the living specimen under study.

Unfortunately, these applications are still way ahead down the road –even though there are some prototypes of optical cryocoolers made at Los Alamos by Epstein and coworkers²⁷– so, in the meantime, a number of research groups are trying to investigate novel materials amenable of efficient laser cooling^{23,24,29,30}. There are two typical probes used in the lab to investigate this phenomenon. On the one hand, in order to probe local or internal cooling, the technique known as collinear photothermal deflection spectroscopy is commonly used. This technique

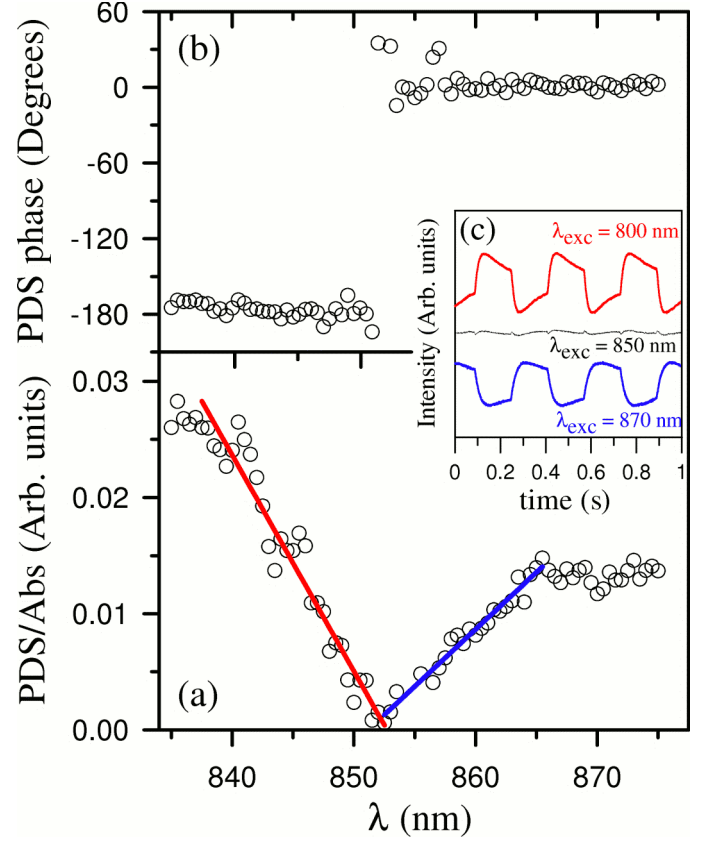


Figure 5: (a) Photothermal signal deflection amplitude normalized by the sample absorption as a function of pumping wavelength for the $\text{Er}^{3+}:\text{KPb}_2\text{Cl}_5$ crystal. (b) Phase of the photothermal deflection signal as a function of pumping wavelength. (c) Photothermal deflection signal waveforms in the heating (800 nm) and cooling (870 nm) regions and around the cooling threshold (850 nm).

is based in the mirage effect, where a probe laser beam probes the thermal lens (an index of refraction gradient) created by a pump laser beam. When the pump laser is adequately tuned so that there is a transition from heating to cooling, there is a change in the direction in which the probe beam deviates. A typical result obtained with the PDS technique can be seen in figure 5 for an Er^{3+} -doped KPC crystal with 0.5% Er when pumping into the $^4\text{I}_{9/2}$ band²⁶. Above the barycenter of this band there is the Stokes region, in which heating occurs. The barycenter appears in that figure as the frequency at which the PDS signal is almost zero. Below this frequency, we enter in the anti-Stokes region, in which cooling occurs. This shows up in the upper panel of that figure as a 180° change in the phase of the PDS signal that clearly indicates the transition from heating to cooling. Also, the transition from heating to cooling can be noticed as the change in sign of the waveforms captured with an oscilloscope, as shown in the (c) panel of figure 5. Furthermore, from the slopes of the PDS signal, one can estimate the cooling efficiency. For this

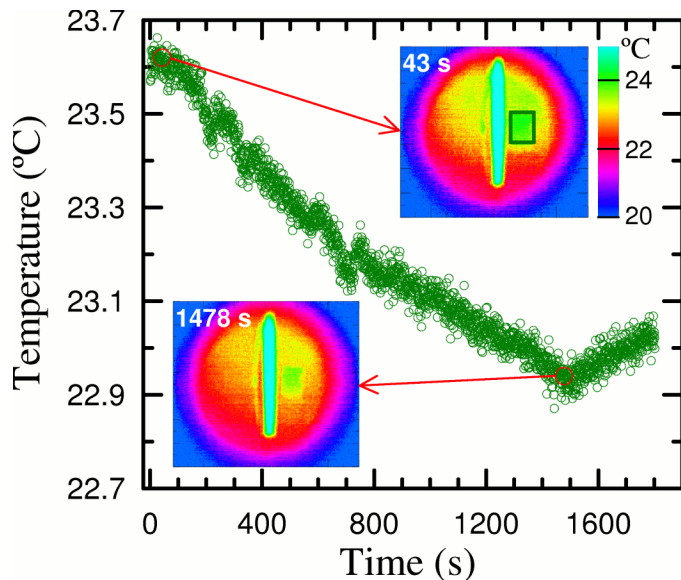


Figure 6: Time evolution of the average temperature of the $\text{Er}^{3+}:\text{KPB}_2\text{Cl}_5$ at 870 nm. The insets show colormaps of the temperature field of the whole system (sample plus cryostat) at two different times as measured with the thermal camera. The rectangle in the upper inset delimits the area used for calculating the average temperature of the sample.

particular system, the cooling efficiency is very small and around 0.4%. On the other hand, in order to probe the presence of macroscopic or bulk cooling—more useful, in fact, for practical applications—commonly an IR thermal camera is used. The typical pictures taken by this device look like the ones shown in the insets of figure 6 for the same sample as before. The figure on the right inset corresponds to an IR picture taken 43 seconds after the laser irradiation of the sample started. The figure on the left inset corresponds to a picture taken after 1483 seconds had passed since laser irradiation started. It can be seen that the color of sample changes between these two instants of time which, according to the color scale, indicates a slight decrease of the temperature of the sample. Actually, it is quite difficult to extract quantitative information from those pictures directly and, therefore, it is better to calculate the average temperature of the sample and represent it as a function of irradiation time, as in the main part of figure 6. It is easy to see that the temperature of the sample dropped by around 0.7°C after 25 minutes of laser irradiation. Interestingly, after those 25 minutes we shut off the laser and this shows up in this figure as an upturn in the temperature of the sample. It is important to stress that, even though it could look like a small temperature change, this is actually quite a good result if one takes into account that there is only a 0.5% Er concentration and no attempt was made to optimize the cooling process.

An interesting fact about these measurements is that there was upconverted emission present during the realization of all these experiments that could be observed

with the naked eye. In order to investigate whether this upconversion played a role in the upconversion process, we used a simple rate equation formalism that has been described elsewhere^{31,32}. The main conclusion coming out from such an analysis is that the efficient upconversion present in these materials provides an additional channel for extracting energy from the system and, therefore, the cooling efficiency increases. Moreover, when upconversion is present, the onset of cooling, that is, the frequency below which cooling occurs, is larger than in the absence of upconversion and, in some limiting cases, there could be cooling even in the Stokes region. The interested reader is referred to those references for more details.

IV. LUMINESCENCE CONTROL WITH PHOTONIC NANOSTRUCTURES

In this section I describe what I think it is the next step into improving the luminescence efficiency of solids and, in particular, the optical cooling efficiency: the use of RE-doped periodic nanoscale photonic heterostructures—also known as photonic crystals—doped with optically active ions for controlling the density of photonic states.

A photonic crystal is an engineered periodic structure made of two or more materials with very different dielectric constants. These photonic nanostructures have generated an ever-increasing interest in the last twenty years because of their potential to control the propagation of light to an unprecedented level^{33,34,35,36,37,38,39,40,41,42,43,44,45,46,47,48,49}. When an electromagnetic wave (EM) propagates in such a structure whose period is comparable to the wavelength of the wave, interesting phenomena occur. Among the most interesting ones are the possibility of forming a complete photonic band gap (CPBG), that is, a frequency range for which no photons having frequencies within that range can propagate through the photonic crystal, to localize light by introducing several types of defects in the lattice, or enhancing certain non-linear phenomena due to small group velocity effects.

More important for our present purpose, a photonic crystal doped with an OAI offers new pathways in which one can improve the luminescence efficiency of the ions embedded in such a structure and, in particular, the cooling efficiency for laser cooling applications: firstly, they allow to control the spontaneous emission of those ions. To see this, one needs to take into account that the probability per unit time of an spontaneous emission of a photon is given by

$$\omega_{sp}(\nu) = \frac{2\pi}{\hbar} |M_{ed}|^2 \text{DOS}(\nu), \quad (2)$$

where M_{ed} is the electric dipole photon-ion coupling and $\text{DOS}(\nu)$ the density of photonic states in which the ion can decay. The important point to notice here is the fact that this emission rate is proportional to the photonic

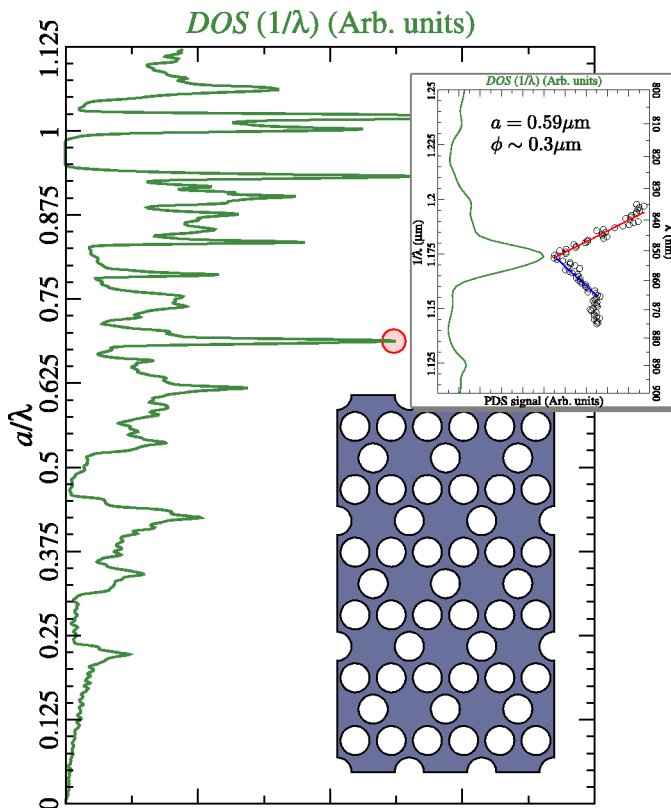


Figure 7: Photonic density of states of a two-dimensional photonic crystal based on an inverse kagomé lattice (bottom inset). The upper inset shows the maximum marked with a small circle for the lattice parameter $a = 590$ nm and diameter of the air holes $\phi = 300$ nm together with the PDS signal for Er-doped KPC crystal.

density of states. In a homogeneous medium, this quantity follows a rather uninteresting power law. However, in a photonic crystal, this is a highly non-trivial quantity that possesses a lot maxima and minima⁵⁰, such as the one shown in figure 7 for a two-dimensional crystal based on an inverse kagomé lattice^{51,52}. The idea is then to adjust the geometrical parameters of the photonic crystal in such a way that one of these maxima coincides with the barycenter of the emitting level of the OAI, so that the power radiated out from the system as spontaneous emission maximizes and so it does the cooling efficiency of the system. For example, in the particular case of the photonic crystal displayed in figure 7, choosing a lattice parameter $a = 590$ nm and a diameter for the air holes $\phi = 300$ nm, we would match one of the maxima in the photonic DOS with the barycenter of the $^4I_{9/2}$ level than can be easily identified in the PDS signal, thus maximizing the spontaneous emission rate of this band.

Secondly, another effect we should take into account is the fact that the constituents of the photonic crystal (dielectric spheres, for example) are of finite size, a few hundred nanometer diameter typically for applications in the visible and near infrared frequency range,

so that this leads to important finite size effects in the phononic density of states. In fact, this has been recently investigated by Ruan and Kaviany⁵³ in RE-doped nanocrystalline powders made of small clusters of diameter around 3 nm. These authors found that the long wavelength region –small energy– of the phonon density of states is enhanced when compared when the corresponding bulk crystal counterpart. This means that we have more phonons of small energy and, therefore, the probability of having an anti-Stokes absorption event increases which, in turn, increases the cooling efficiency. Given the similarity between the systems analyzed by Ruan and Kaviany and the photonic crystals considered in this work with regards to the finite size of the constituents, one can expect that a similar line of reasoning applies to these later structures.

Finally, we could also use point defects introduced in a controlled way into the photonic crystal to improve the cooling efficiency. It is well known that light tends to localize around these defects in the presence of a complete photonic band gap³³. As a consequence, the effective interaction time between the light and the OAI increases and so it does the total probability of having an anti-Stokes absorption event. Actually, Ruan and Kaviany found that light localization in RE-doped powders (due to a different physical phenomenon than the one considered here) by itself is responsible for an enhancement of about a 100% of the cooling efficiency⁵³.

Of course, the best route to maximize the enhancement of the cooling efficiency due to these effects is to take all of them into account at the same time. That is a venue of research that our group is currently pursuing.

V. CONCLUSIONS

As mentioned in the introduction, this manuscript summarizes three years of research carried out by our group in the field of the optical spectroscopy of Er-doped low-phonon potassium lead halides. The results presented here clearly show that these materials are very promising for ir-to-vis upconversion applications: their small phonons make upconversion very efficient in these systems, they exhibit a wealth of upconversion mechanisms so that the dynamics is complex in spite of their relative simplicity, and the type of dynamics can be easily selected by adequately tuning the pumping laser frequency.

I have also described how one can use conventional optical processes (anti-Stokes absorption) for non-conventional applications: laser cooling of luminescent solids. Indeed, potassium lead chloride is a very useful host material for this type of applications due to its extremely small phonons. In the past, we demonstrated laser cooling in an Yb^{3+} -doped KPC crystal²⁹. More recently, we demonstrated laser cooling in an Er^{3+} -doped KPC crystal²⁶, with the special significance this has for potential applications in the field of optical telecommuni-

cations and for bioimaging and phototherapy. This later result is briefly described here together with a novel up-conversion cooling mechanism we have recently identified.

Finally, I have made a discursion into –what I consider– is the logical next step in the field of optical spectroscopy of condensed phases: controlling the luminescence efficiency by using photonic nanoscale heterostructures as host materials for optically active ions. I have used the cooling efficiency as a guiding example of this idea and I have explained the different ways in which this quantity can be enhanced by using a photonic crystal doped with optically active ions: control of the spontaneous emission rate of the optically active ion by means of the photonic density of states of the photonic crystal, enhancement of the phononic density of states in the long wavelength region due to the finite size of the constituents of the photonic crystal, and introduction of point defects in a controlled way to localize light around them.

I hope these pages serve the purpose of motivating other researchers to further explore these ideas so we can advance into this new era of the optical spectroscopy in which not only will we be able to understand the optical properties of the condensed phases but also to tailor them for specific applications.

Acknowledgments

I got acquainted with Professor Michael Sturge's works when, as a graduate student, I was working on elucidat-

ing the mechanisms responsible for the anomalous low-temperature behavior of the homogeneous linewidths of amorphous solids doped with optically active ions. I admired the well reputed scientist that, among other contributions, settled the foundations that allowed us to understand this phenomenon. It is thus easy to understand the great and unexpected honor it has been for me to receive this prize named after him. Obviously, there have been many people that helped me during these long years: Joaquín Fernández, Rolindes Balda, and all my colleagues at the Dpto. de Física Aplicada I, Miguel Angel Cazalilla, Dave Huber, Steve Conradson, and Bill Yen –a very special friend. But, above all of them, I would like to dedicate this prize to my wife, who has given me love and support during all these years.

Of course, the results presented in this manuscript are not the work of a single person. Rather, they are the outcome of a strong collaboration between Joaquín Fernández, Rolindes Balda, and myself at the Dpto. de Física Aplicada I of the E.T.S. de Ingeniería de Bilbao. Joaquín and Rolindes have carried out the hard experimental work described above and to them goes my gratitude for this and for the many things I have learned from them through the years.

Finally, I acknowledge financial support from the Spanish Ministerio de Educación y Ciencia under the Ramón y Cajal program.

* Electronic address: angel.garcia-adeva@ehu.es

- ¹ W. Length and R. M. McFarlane, *Opt. Photonics News* **3**, 8 (1992).
- ² T. Sandrock, H. Scheife, E. Heumann, and G. Huber, *Opt. Lett.* **22**, 808 (1997).
- ³ R. J. Thrash and L. F. Johnson, *J. Opt. Soc. Am. B* **11**, 881 (1994).
- ⁴ R. Paschotta, P. R. Barber, A. C. Tropper, and D. C. Hanna, *J. Opt. Soc. Am. B* **14**, 1213 (1997).
- ⁵ P. E.-A. Möbert, A. Diening, E. Heumann, G. Huber, and B. H. T. Chai, *Laser Phys.* **8**, 210 (1998).
- ⁶ A. Pollack and D. B. Chang, *J. Appl. Phys.* **64**, 2885 (1988).
- ⁷ M. P. Hehlen, K. Krämer, H. U. Güdel, R. A. McFarlane, and R. N. Schwartz, *Phys. Rev. B* **49**, 12475 (1994).
- ⁸ M. P. Hehlen, G. Frei, and H. U. Güdel, *Phys. Rev. B* **50**, 16264 (1994).
- ⁹ T. Riedener, P. Egger, J. Hulliger, and H. U. Güdel, *Phys. Rev. B* **56**, 1800 (1997).
- ¹⁰ N. J. Cockroft, G. D. Jones, and D. C. Nguyen, *Phys. Rev. B* **45**, 5187 (1992).
- ¹¹ R. Burlot-Loison, M. Pollnau, K. Kramer, P. Egger, J. Hulliger, and H. U. Güdel, *J. Opt. Soc. Am. B* **17**, 2055 (2000).
- ¹² R. Balda, A. J. Garcia-Adeva, M. Voda, and J. Fernández,

- Phys. Rev. B* **69**, 205203 (2004).
- ¹³ A. J. Garcia-Adeva, R. Balda, J. Fernandez, E. E. Nyein, and U. Hömmerich, *Phys. Rev. B* **72**, 165116 (2005).
- ¹⁴ M. C. Nostrand, R. H. Page, S. A. Payne, W. F. Krupke, P. G. Schunemann, and L. I. Isaenko, *OSA Trends Opt. Photonics Ser.* **19**, 524 (1998).
- ¹⁵ L. I. Isaenko, A. P. Yelisseyev, V. A. Nadolinny, V. I. Pashkov, M. C. Nostrand, R. H. Page, S. A. Payne, and R. Solarz, *Proc. SPIE* **3265**, 242 (1998).
- ¹⁶ M. C. Nostrand, R. H. Page, S. A. Payne, W. F. Krupke, P. G. Schunemann, and L. I. Isaenko, *OSA Trends Opt. Photonics Ser.* **26**, 441 (1999).
- ¹⁷ R. Balda, J. Fernández, A. Mendioroz, M. Voda, and M. Al-Saleh, *Phys. Rev. B* **68**, 165101 (2003).
- ¹⁸ A. Mendioroz, R. Balda, M. Voda, M. Al-Saleh, and J. Fernández, *Opt. Mater.* **26**, 251 (2004).
- ¹⁹ K. Rademaker, W. F. Krupke, R. H. Page, S. A. Payne, K. Petermann, G. Huber, A. P. Yelisseyev, L. I. Isaenko, U. N. Roy, A. Burger, K. C. Mandal, and K. Nitsch, *J. Opt. Soc. Am. B* **21**, 2117 (2004).
- ²⁰ U. Hömmerich, E. E. Nyein, and S. B. Trivedi, *J. Lumin.* **113**, 100 (2005).
- ²¹ T. Riedener and H. U. Güdel, *J. Chem. Phys.* **107**, 2169 (1997).
- ²² A. Kastler, *J. Phys. Radium* **11**, 255 (1950).

- ²³ R. I. Epstein, M. I. Buchwald, B. C. Edwards, T. R. Gosnell, and C. E. Mungan, *Nature* (London) **377**, 500 (1995).
- ²⁴ C. W. Hoyt, M. Sheik-Bahae, R. I. Epstein, B. C. Edwards, and J. E. Anderson, *Phys. Rev. Lett.* **85**, 3600 (2000).
- ²⁵ J. Fernandez, A. Mendioroz, A. J. Garcia, R. Balda, and J. L. Adam, *Phys. Rev. B* **62**, 3213 (2000).
- ²⁶ J. Fernandez, A. J. Garcia-Adeva, and R. Balda, *Phys. Rev. Lett.* **97**, 033001 (2006).
- ²⁷ B. C. Edwards, M. I. Buchwald, and R. I. Epstein, *Rev. Sci. Instr.* **69**, 2050 (1998).
- ²⁸ B. C. Edwards, M. I. Buchwald, and R. I. Epstein, *Optical refrigerator using reflectivity tuned dielectric mirrors*, United States Patent number 6041610, 2000.
- ²⁹ A. Mendioroz, J. Fernandez, M. Voda, M. Al-Saleh, R. Balda, and A. J. Garcia-Adeva, *Opt. Lett.* **27**, 1525 (2002).
- ³⁰ J. Fernandez, A. Mendioroz, A. J. Garcia, R. Balda, and J. L. Adam, *J. Alloys Compd.* **323-324**, 239 (2001).
- ³¹ A. J. Garcia-Adeva, R. Balda, and J. Fernandez, *Proc. of the SPIE* **6461**, 646102 (2007).
- ³² A. J. Garcia-Adeva, R. Balda, and J. Fernandez, *Proc. of the SPIE* **6469**, 64690F (2007).
- ³³ J. D. Joannopoulos, R. D. Meade, and J. N. Winn, *Photonic Crystals: Molding the Flow of Light* (Princeton University Press, Singapore 1999).
- ³⁴ S. G. Johnson and J. D. Joannopoulos, *Photonic Crystals: The Road from Theory to Practice* (Luwer Academic Publishers, London 2003).
- ³⁵ S. John, *Phys. Rev. Lett.* **58**, 2486-2489 (1987).
- ³⁶ E. Yablonovitch, *Phys. Rev. Lett.* **58**, 2059-2062 (1987).
- ³⁷ E. Yablonovitch and T. J. Gmitter, *Phys. Rev. Lett.* **63**, 1950 (1989).
- ³⁸ K. M. Ho, C. T. Chan, and C. M. Soukoulis, *Phys. Rev. Lett.* **65**, 3152-3155 (1990).
- ³⁹ J. Martorell and N. M. Lawandy, *Phys. Rev. Lett.* **65**, 1877 (1990).
- ⁴⁰ C. T. Chan, K. M. Ho, and C. M. Soukoulis, *Europhys. Lett.* **16**, 563 (1991).
- ⁴¹ E. Yablonovitch, T. J. Gmitter, and K. M. Leung, *Phys. Rev. Lett.* **67**, 2295 (1991).
- ⁴² R. D. Meade, K. D. Brommer, A. M. Rappe, J. D. Joannopoulos, *Phys. Rev. B* **44**, 10961 (1991).
- ⁴³ R. D. Meade, K. D. Brommer, A. M. Rappe, and J. D. Joannopoulos, *Appl. Phys. Lett.* **61**, 495 (1992).
- ⁴⁴ E. Chow et al., *Nature* **407**, 983-986 (2000).
- ⁴⁵ J. D. Joannopoulos, *Nature* **414**, 257-258 (2001).
- ⁴⁶ K. Sakoda, *Optical Properties of Photonic Crystals* (Springer, Heidelberg 2001).
- ⁴⁷ J. W. Fleischer, M. Segev, N. K. Efremidis, and D. N. Christodoulides, *Nature* **422**, 147-150 (2003).
- ⁴⁸ Y. Akahane, T. Asano, B. S. Song, and S. Noda, *Nature* **425**, 944-947 (2003).
- ⁴⁹ M. Soljacic and J. D. Joannopoulos, *Nature Materials* **3**, 211-219 (2004).
- ⁵⁰ A. J. Garcia-Adeva, *Phys. Rev. B* **73**, 073107 (2006).
- ⁵¹ A. J. Garcia-Adeva, R. Balda, and J. Fernandez, *Opt. Mat.* **27**, 1733 (2005).
- ⁵² A. J. Garcia-Adeva, *New J. Phys.* **8**, 86 (2006).
- ⁵³ X. L. Ruan and M. Kaviany, *Phys. Rev. B* **73**, 155422 (2006).